HHS Public Access

Author manuscript

Gastroenterology. Author manuscript; available in PMC 2020 September 01.

Published in final edited form as:

Gastroenterology. 2019 September ; 157(3): 793–806.e14. doi:10.1053/j.gastro.2019.05.066.

Aryl Hydrocarbon Receptor Signaling Prevents Activation of Hepatic Stellate Cells and Liver Fibrogenesis in Mice

Jiong Yan[1,#], **Hung-Chun Tung**[1,#], **Sihan Li**[1], **Yongdong Niu**[1], **Wojciech G. Garbacz**[1], **Peipei Lu**[1], **Yuhan Bi**[1], **Yanping Li**[3], **Jinhan He**[3], **Meishu Xu**[1], **Songrong Ren**[1], **Satdarshan P. Monga**[4], **Robert F. Schwabe**[5], **Da Yang**[1], **Wen Xie**[1,2]

[1]Center for Pharmacogenetics and Department of Pharmaceutical Sciences, University of Pittsburgh, Pittsburgh, PA, USA

[2]Department of Pharmacology and Chemical Biology, University of Pittsburgh, Pittsburgh, PA, USA

[3]Department of Pharmacy, West China Hospital, Sichuan University, Chengdu, Sichuan, China

[4]Department of Pathology and Medicine, University of Pittsburgh School of Medicine, Pittsburgh, PA, USA

[5]Department of Medicine, Columbia University, New York, NY, USA

Abstract

Background & Aims: The role of aryl hydrocarbon receptor (AHR) in liver fibrosis is controversial, because loss and gain of AHR activity each lead to liver fibrosis. The goal of this study is to investigate how the expression of AHR by different liver cell types, hepatic stellate cells (HSCs) in particular, affects liver fibrosis in mice.

Methods: We studied the effects of AHR on primary mouse and human HSCs, measuring their activation and stimulation of fibrogenesis using RNA-seq analysis. C57BL/6J mice were given the AHR agonists TCDD or ITE, or carbon tetrachloride (CCl_4), or underwent bile duct ligation. We also performed studies in mice with disruption of *Ahr* specifically in HSCs, hepatocytes, or Kupffer cells. Liver tissues were collected from mice and analyzed by histology, immunohistochemistry, and immunoblotting.

Results: AHR was expressed at high levels in quiescent HSCs, but the expression decreased with HSC activation. Activation of HSCs from AHR-knockout mice was accelerated, compared to HSCs from wild-type mice. In contrast, TCDD or ITE inhibited spontaneous and transforming

Correspondence: Dr. Wen Xie, 306 Salk Pavilion, University of Pittsburgh, Pittsburgh, PA 15261. wex6@pitt.edu.

Author contributions: W.X. conceived and mentored this study. J.Y., and H.T. designed and performed experiments, acquired and analyzed data, and wrote the draft of the manuscript. H.T., S.L., Y.N., P.L., Y.B., and M.X. performed experiments. Y.N., W.G.G., P.L., J.H., M.X., S.R., S.P.M., R.F.S., and D.Y. gave technical support and conceptual advice. W.X., J.Y., and H.T. wrote the manuscript.

[#]These authors contributed equally to this work

Disclosures: The authors have declared that there is no conflict of interest.

growth factor beta (TGFB)-induced activation of HSCs. Mice with disruption of *Ahr* in HSCs, but not hepatocytes or Kupffer cells, developed more severe fibrosis following administration of CCl_4 or bile duct ligation. C57BL/6J mice given ITE did not develop CCl_4-induced liver fibrosis, whereas mice without HSC AHR given ITE did develop CCl_4-induced liver fibrosis. In studies of mouse and human HSCs, we found that AHR prevents TGFB-induced fibrogenesis by disrupting the interaction of SMAD3 with beta-catenin, which prevents the expression of genes that mediate fibrogenesis.

Conclusions: In studies of human and mouse HSCs, we found that AHR prevents HSC activation and expression of genes required for liver fibrogenesis. Development of non-toxic AHR agonists or strategies to activate AHR signaling in HSCs might be developed to prevent or treat liver fibrosis.

Graphical Abstract

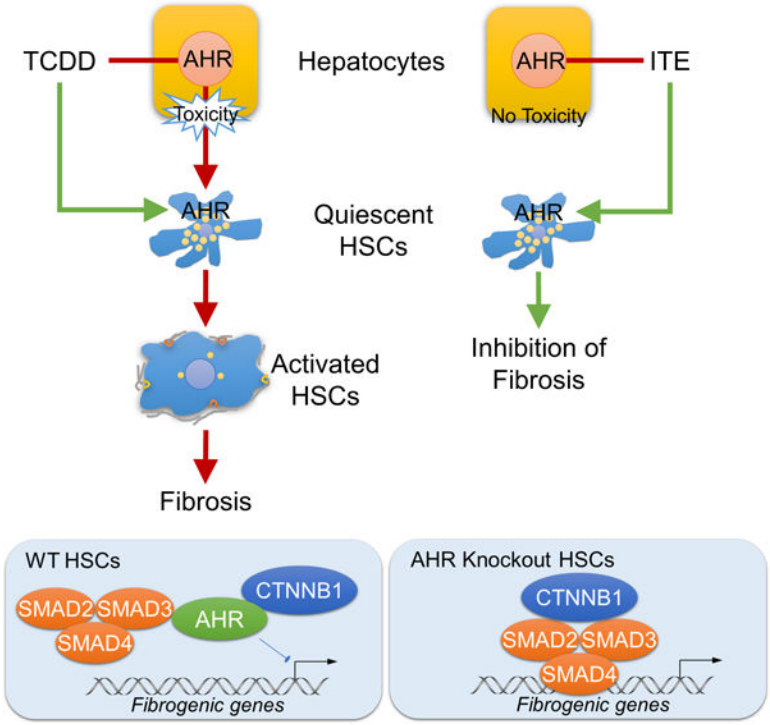

Lay Summary

Activation of hepatic stellate cells (HSCs) is key to liver fibrosis formation. This study showed that drug activation of the aryl hydrocarbon receptor can prevent HSC activation and liver fibrosis.

Keywords

gene regulation; signal transduction; cell-specific effect; xenobiotic receptor

Introduction

Liver fibrosis, defined as the excessive intercellular accumulation of extracellular matrix (ECM) proteins in the liver, is strongly associated with chronic viral or non-viral liver injuries.[1] Advanced liver fibrosis causes liver cirrhosis, leading to portal hypertension and liver failure. Liver fibrosis is also a major risk factor for the development of hepatocellular carcinoma. Activated hepatic stellate cells (HSCs) are the major cell population responsible for the production of ECM proteins and pro-fibrogenic cytokines.[2] Residing in the space of Disse between the sinusoidal endothelial cells and hepatocytes, HSCs are characterized by their expression of desmin and glial fibrillary acidic protein in the quiescent state and α-smooth muscle actin (α-SMA) in the activated state. The activation of HSCs, which is characterized by increased fibrogenic gene expression and proliferation, is central to the pathogenesis of liver fibrosis. As such, understanding the molecular basis of HSC activation will help to develop strategies to prevent and treat liver fibrosis. The TGFβ pathway that integrates a myriad of injury signals is pivotal for HSC activation.[3] Emerging evidence also suggested the role of Wnt-β-catenin signaling in promoting HSC activation and its crosstalk with the TGFβ pathway in the fibrotic diseases.[4] However, how Wnt signaling, particularly the β-catenin-mediated canonical pathway, promotes the fibrogenic progression is not fully understood.

The aryl hydrocarbon receptor (AhR), highly expressed in the liver, is a well-established xenobiotic receptor that senses environmental toxicants and regulates xenobiotic metabolism.[5] Many industrial pollutants, such as the polycyclic aromatic hydrocarbons, are AhR ligands.[6] 2,3,7,8-tetrachlorodibenzo-*p*-dioxin (TCDD), a prototypical xenobiotic activator of AhR, is a tool compound widely used to study the toxicological effect of AhR. As a ligand-dependent transcriptional factor, AhR signals through its DNA-binding motif and diverse protein partners.[6] Upon binding by TCDD, AhR translocates into the nucleus where it heterodimerizes with AhR nuclear translocator (ARNT) on the xenobiotic response elements (XREs) to regulate the transcription of a battery of TCDD-responsive genes involved in xenobiotic catabolism, inflammatory response, and metabolic reprogramming. ChIP-sequencing analysis has revealed non-XRE binding of AhR in the genome, suggesting AhR responsive genes are not limited to those harboring XREs.[7] Subsequent studies, mainly through the characterization of $AhR^{-/-}$ mice, have implicated AhR and its endogenous ligands in tissue development and pathophysiology, including liver fibrosis.[8, 9] The AhR signaling has also been implicated in the homeostasis of energy metabolism, gut microbiota, stem cell differentiation, circadian rhythm, and adaptive immunity.[10] In addition to its function as a transcriptional factor, AhR also participates in the proteasome-dependent proteolysis by functioning as a substrate-specific adaptor that targets selected proteins for degradation in the Cullin4B (CUL4B) ubiquitin E3 ligase complex $CUL4B^{AhR}$.[11] The reported substrate proteins for $CUL4B^{AhR}$ include estrogen receptor α, androgen receptor, and β-catenin.[11, 12]

The role of AhR in liver fibrosis has been intriguing and controversial. On one hand, $AhR^{-/-}$ mice exhibited spontaneous liver fibrosis.[8] On the other hand, treatment of mice with TCDD or constitutive activation of AhR in the hepatocytes sensitized mice to methionine and choline deficient- or high-fat diet induced liver fibrosis.[13–15] The liver is an organ of

multiple cell types, including the hepatocytes, HSCs and Kupffer cells. It is unclear whether AhR has a cell-type specific role in liver fibrosis. More specifically, it has not been reported whether and how AhR plays a role in HSC activation and liver fibrosis.

In this study, we uncovered an unexpected role of AhR in preventing HSC activation and attenuating liver fibrosis. Knockout of AhR in HSCs was sufficient to cause spontaneous liver fibrosis and sensitize mice to experimental liver fibrosis. In contrast, the non-toxic AhR agonist ITE exhibited anti-fibrotic activity in vivo.

Materials and Methods

Detailed information of chemical reagents, antibodies, and real-time PCR primers is provided in Supplementary Tables 1–3.

Experimental Animals and Histology

The wildtype C57BL/6J (000664), $AhR^{fl/fl}$ ($Ahr^{tm3.1Bra}$/J, 006203), Albumin-Cre (B6.Cg-Tg(Alb-cre)21Mgn/J, 003574), and LysM-Cre (B6.129P2-$Lyz2^{tm1(cre)Ifo}$/J, 004781) mice were purchased from the Jackson Laboratory (Bar Harbor, ME). Lrat-Cre mice were previously described.[2] $AhR^{fl/fl}$ mice were crossbred with Albumin-Cre, LysM-Cre, or Lrat-Cre mice to generate cell type-specific AhR knockout mice. For the toxicological comparison of TCDD and ITE, 6 week old male C57BL/6J mice were treated with vehicle (DMSO), TCDD (25 μg/kg), or ITE (10 mg/kg) once a week for two weeks by intraperitoneal injection. The animals were terminated 6 h after the third injection. For the carbon tetrachloride (CCl_4) model of liver fibrosis, 9–10 week old male mice were intraperitoneally injected with CCl_4 (1 μl/g body weight, 1:3 diluted in corn oil, twice a week) for 4 weeks. The animals were terminated 72 h after the final CCl_4 injection. When ITE was used to treat CCl_4-induced liver fibrosis, ITE (10 mg/kg) was administrated every other day along with CCl_4 (0.5 μl/g body weight) in corn oil by intraperiton eal injection for 4 weeks. The animals were terminated 6 h after the final dose of ITE. For the bile duct ligation (BDL) model of liver fibrosis, 8–9 week old mice were subject to common bile duct ligation, and the animals were terminated 14 days after the surgery. See Supplementary Information for details of the histology. The use of mice was in accordance with the University of Pittsburgh Institutional Animal Care and Use Committee.

Primary HSC Isolation and Sorting, Adenovirus, Lentivirus, Plasmids and Cell Transfection

Primary mouse HSCs were isolated as previously reported.[16] For the RNA-seq analysis, HSCs were further purified by vitamin A-based FACS sorting as described.[16] See Supplementary Information for details of primary HSCs isolation and sorting, adenovirus, lentivirus, plasmids and cell transfection.

RNA Sequencing (RNA-seq) Analysis

RNA-seq was performed at the Health Sciences Sequencing Core at Children's Hospital of Pittsburgh. Gene expression was analyzed by gene set enrichment analysis (GSEA).[17] See Supplementary Information for details of bioinformatic analysis of the RNA-seq results and the Gene Expression Omnibus (GEO) datasets.

Immunofluorescence, Immunoprecipitation (IP) and Western Blot, Chromatin Immunoprecipitation (ChIP), and Quantitative Real-Time PCR

These were performed as described,[18] and see Supplementary Information for details.

Statistics

Statistical analysis was performed using Prism GraphPad 7.0 (La Jolla, CA). All results were presented as means ± SEM of at least three replicates. Statistical differences between groups were determined using unpaired two-tailed Student *t* test or one-way ANOVA with post-hoc Tukey test. P values less than 0.05 were considered statistically significant.

Results

Treatment of mice with the non-toxic AhR ligand ITE ameliorates CCl_4-induced liver fibrosis

The classical AhR ligand TCDD induces liver fibrosis in mice.[14] TCDD is known to be toxic to the liver, so we speculated that the liver fibrosis might have been secondary to the TCDD-induced hepatotoxicity and inflammation. We decided to test the effect of 2-(1'H-indole-3'-carbonyl)-thiazole-4-carboxylic acid methyl ester (ITE), a non-toxic tryptophan metabolite and endogenous AhR agonist,[19] on liver fibrosis. Treatment of mice with TCDD for 2 weeks caused typical hepatotoxicity as indicated by neutrophil infiltration and collagen deposition (Figure 1*A*), consistent with a previous report.[20] In contrast, the liver of ITE-treated mice showed no signs of hepatotoxicity and fibrosis (Figure 1*A*). The lack of fibrogenic activity of ITE was confirmed by measuring the expression of fibrogenic marker genes (Figure 1*B*). We then tested the effect of ITE on CCl_4-induced liver fibrosis as outlined in Figure 1*C*. Treatment with ITE ameliorated CCl_4-induced liver fibrosis, which was supported by decreased collagen deposition and fibrogenesis as revealed by Masson's Trichrome staining (MTS), Sirius Red staining, and immunostaining of α-SMA (Figure 1*D*). The suppression of α-SMA in ITE- and CCl_4-treated mice was further verified by Western blotting (Figure 1*E*) and real-time PCR (Figure 1*F*). Consistent with the relief of liver fibrosis, the levels of ALT and AST were decreased in ITE-treated mice compared to their vehicle-treated counterparts (Figure 1*G*). The hepatic expression of *Cyp1a1* and *Cyp1a2*, two typical AhR target genes, was induced by ITE, suggesting AhR was efficiently activated (Figure 1*H*). We also determined whether ITE can mitigate the existing liver fibrosis by treating mice with ITE after the initiation of the CCl_4 model as outlined in Supplementary Figure 1*A*. The post-treatment with ITE also attenuated CCl_4-induced liver fibrosis as shown by histology (Supplementary Figure 1*B*) and measurement of α-SMA protein expression (Supplementary Figure 1*C*). ITE post-treatment induced the expression of *Cyp1a1* and *Cyp1a2* (Supplementary Figure 1*D*), but had little effect on the serum ALT and AST levels (Supplementary Figure 1*E*).

AhR is highly expressed in HSCs and the expression of AhR inversely correlates with HSC activation in vitro and in vivo

To investigate whether AhR in the HSCs mediates the anti-fibrotic effect of ITE, we compared the expression of AhR in primary hepatocytes and HSCs isolated from the same

mice. There was an approximately 4-fold increase in the mRNA expression of both *Ahr* and its DNA-binding partner *Arnt* in HSCs compared to hepatocytes (Figure 2*A*). The basal expression of *Cyp1a1* and *Cyp1b1* was also markedly higher in HSCs (Figure 2*A*). These results were consistent with a recently reported proteomic analysis, in which HSCs were shown to express a higher level of AhR than hepatocytes.[21] Treatment of primary HSCs isolated from WT mice with TCDD induced the expression of *Cyp1a1*, *Cyp1a2* and *Cyp1b1*, but the induction was abolished in HSCs isolated from $AhR^{-/-}$ mice (Figure 2*B*), suggesting that AhR in HSCs is transcriptionally functional. Moreover, we found the expression of AhR was inversely correlated with the activation of HSCs. When primary HSCs were subject to spontaneous activation in culture, the expression of *AhR* and its target gene *Cyp1a1* in primary mouse (Figure 2*C*) and human (Figure 2*D*) HSCs decreased with the onset of HSC activation in a time-dependent manner. The expression of *Acta2* was measured to validate the HSC activation. Interestingly, we observed a major induction of *Cyp1b1*, another AhR target gene, with the onset of HSC activation (Supplementary Figure 2), suggesting that it was not a general decline in drug metabolism adipogenic differentiation in fully activated HSCs was correlated with an increased expression of AhR (Supplementary Figure 3).

The fibrosis-responsive down-regulation of AhR in HSCs was also confirmed in vivo, as the primary HSCs isolated from CCl_4-treated mice showed a decreased expression of *Ahr* compared to HSCs isolated from vehicle-treated mice (Figure 2*E*). Moreover, analysis of two Gene Expression Omnibus (GEO) datasets, alcoholic hepatitis (GSE28619) and cirrhosis (GSE89377), revealed that both fibrosis-prone liver diseases are associated with a decreased expression of *AHR* and its target gene *CYP1A2* (Figure 2*F*), suggesting that the fibrosis-responsive down-regulation of AHR is conserved in humans.

Pharmacological activation or forced expression of AhR inhibits HSC activation

To determine whether the dynamic expression of AhR during HSC activation is functionally relevant, we treated primary mouse HSCs with TCDD and found it inhibited the expression of fibrogenic genes at both the protein (Figure 3*A*) and mRNA (Figure 3*B*) levels. The activation of AhR by TCDD was verified by the induction of *Cyp1b1* (Supplementary Figure 4*A*). Treatment of primary mouse HSCs with 6-formylindolo[3,2-b]carbazole (FICZ) and ITE, two endogenous AhR agonists, also inhibited fibrogenic gene expression (Supplementary Figure 4*B*). TCDD or ITE had little effect on HSC proliferation and apoptosis, as shown by BrdU labeling (Supplementary Figure 4*C*) and TUNEL staining (Supplementary Figure 4*D*), respectively. The inhibitory effect of TCDD on HSC activation was AhR-dependent, because the inhibitory effect was abolished in HSCs isolated from $AhR^{-/-}$ mice, as evaluated by cell morphology (Figure 3*C*), or the expression of fibrogenic marker genes (Figure 3*D*). A similar pattern of inhibition was observed in primary human HSCs treated with the human AHR activator 3-methylcholanthrene (3MC) (Figure 3*E*). The activation of AHR by 3MC was verified by the induction of *CYP1A2* (Supplementary Figure 4*E*). Inhibition of HSC activation was also observed in primary mouse HSCs infected with adenovirus expressing the mouse AhR (Ad-AhR), as shown by the immunofluorescence of α-SMA and Ki67 (Figure 3*F*) and the expression of fibrogenic genes (Figure 3*G*). Adenoviral overexpression of AhR achieved a similar inhibition of human HSC activation (Figures 3*H* and *I*). The adenoviral overexpression of AhR and

induction of AhR target genes in the mouse (Supplementary Figure 4*F*) and human (Supplementary Figure 4*G*) HSCs was validated by real-time PCR.

Knockout of AhR promotes HSC activation in vitro

Consistent with our hypothesis that the down-regulation of AhR contributes to the activation of HSCs, HSCs isolated from $AhR^{-/-}$ mice showed enhanced culture-induced activation as shown by cell morphology (Figure 4*A*) and induction of fibrogenic marker genes (Figure 4*B*). Increased protein expression of α-SMA and Col1A1 in $AhR^{-/-}$ HSCs was verified by Western blotting (Figure 4*C*), and induction of α-SMA and Ki67 was verified by immunofluorescence (Figure 4*D*).

To better assess the effect of AhR knockout on HSC activation, we performed RNA-seq analysis on primary HSCs isolated from WT and $AhR^{-/-}$ mice following vitamin A autofluorescence-based FACS.[16] The RNA-seq results are shown in Supplementary Table 4, with the major pathways affected presented in Supplementary Figure 5*A*. $AhR^{-/-}$ HSCs exhibited altered transcriptome including an elevated expression of fibrogenic markers, such as *Col1a1*, *Col1a2*, *Col3a1* and *Lox* (Figure 4*E*). Several pathways related to HSC activation were selected for Gene Set Enrichment Analysis (GSEA).[17] We found a significant up-regulation of "Extracell ular Matrix," "Cell Proliferation," "Cytokine Receptor B inding," and "Wnt Signaling Pathway" in $AhR^{-/-}$ HSCs (Figure 4*F*). The "Cell Cycle Progression Pathways" were also si gnificantly up-regulated, whereas "TGF β Pathway" and "Epithelial Mesenchymal Transition" showed a trend of increase (Supplementary Figure 5*B*). Overall, the RNA-seq results supported the notion that $AhR^{-/-}$ HSCs were activated with an elevated Wnt signaling. When the RNA-seq results were integrated with a previously reported AHR-binding element (dioxin responsive element, or DRE) database,[33] we found that 4901 out of 17128 genes have at least one potential DRE (Supplementary Table 5), but the DRE-harboring genes are not enriched in either up-regulated or down-regulated gene sets (Supplementary Table 6). It was also noted that many of the fibrogenic genes, such as *Col1a2*, do not contain DREs. The activation of $AhR^{-/-}$ HSCs was attenuated when the expression of AhR was reconstituted by adenoviral infection, as shown by the protein expression of α-SMA and Col1A1 (Figure 4*G*), the mRNA expression of fibrogenic genes (Figure 4*H*), and immunofluorescence of α-SMA and Ki67 (Figure 4*I*).

Knockout of AhR in HSCs sensitizes mice to liver fibrosis and abolishes the anti-fibrotic activity of ITE

To determine whether AhR suppresses HSC activation and fibrosis in vivo, we generated HSC-specific AhR knockout mice (HSC-KO) by crossbreeding the AhR floxed ($AhR^{fl/fl}$, flox) mice[20] with the Lrat-Cre transgenic mice expressing Cre in HSCs under the control of the lecithin-retinol acyltransferase (Lrat) gene promoter[2] (Supplementary Figure 6*A*). The AhR expression in HSCs isolated from HSC-KO mice was decreased by 75% compared to the flox mice (Supplementary Figure 6*B*). Compared to the flox mice, HSC-KO mice exhibited more pronounced liver fibrosis when challenged with CCl_4, as evidenced by increased collagen deposition and expression of α-SMA and Desmin (Figure 5*A*). The increased protein expression of α-SMA (Figure 5*B*) and mRNA expression of collagen genes (Figure 5*C*) in HSC-KO mice were verified by Western blotting and real-time PCR,

respectively. The HSC-KO mice also exhibited increased sensitivity to bile duct ligation (BDL)-induced liver fibrosis, as evidenced by increased expression of α-SMA (Supplementary Figure 6*C*) and histological analysis (Supplementary Figure 6*D*), but without affecting the serum ALT and AST levels (Supplementary Figure 6*E*). Furthermore, the anti-fibrotic effects of ITE were abolished in HSC-KO mice as shown by histology (Figure 5*D*), fibrogenic gene expression (Figure 5*E*), and serum ALT and AST levels (Figure 5*F*), suggesting the HSC AhR is required for the anti-fibrotic activity of ITE.

To determine whether the hepatocyte AhR plays a role in the development of liver fibrosis, we also generated the hepatocyte-specific AhR knockout mice (HEP-KO) by crossbreeding the AhR floxed mice with the Albumin-Cre transgenic mice (Supplementary Figure 6*F*). Compared to flox mice, HEP-KO mice showed a similar sensitivity to CCl_4-induced liver fibrosis (Supplementary Figure 6*F*).

It has been reported that the whole body $AhR^{-/-}$ mice exhibited spontaneous periportal liver fibrosis[8, 9] which was verified by our own analysis (Supplementary Figure 7). To determine the loss of AhR in which cell type is responsible, we used the HEP-KO and HSC-KO mice as well as the Kupffer cell-specific AhR knockout mice (MAC-KO). The MAC-KO mice were generated by crossbreeding the AhR floxed mice with the LysM-Cre transgenic mice. Compared to the whole body $AhR^{-/-}$ mice, only HSC-KO mice, but not HEP-KO or MAC-KO mice, showed spontaneous liver fibrosis as shown by Sirius Red staining and immunostaining of α-SMA (Supplementary Figure 7).

AhR attenuates TGFβ-stimulated fibrogenesis by inhibiting Smad3-mediated transcriptional activation of fibrogenic genes

The TGFβ-Smad3 signaling stimulates liver fibrogenesis and is central to HSC activation. Indeed, we showed the recruitment of pSmad3 onto the *Acta2* and *Col1a1* gene promoters was increased in CCl_4-treated liver (Supplementary Figure 8*A*, left panel). Moreover, the CCl_4-responsive recruitment of pSmad3 onto the *Acta2* gene promoter was inhibited by the co-treatment of ITE (Supplementary Figure 8*A*, right panel). Having shown the inhibitory effect of AhR on the spontaneous activation of HSCs, we went on to determine whether AhR can also inhibit TGFβ-stimulated HSC activation. Treatment of primary mouse HSCs with TGFβ induced the expression of fibrogenic genes as expected, but the inductions were largely attenuated by the co-treatment of TCDD (Figure 6*A*). The attenuation of TGFβ-induced expression of α-SMA by TCDD was confirmed by immunofluorescence (Figure 6*B*). Next, we overexpressed AhR in the human stellate cell line LX2 in which the endogenous AhR had little expression and little response to AhR ligands, whereas overexpression of AhR restored the responsiveness to AhR ligands (Supplementary Figure 8*B*). Overexpression of AhR in LX2 cells significantly attenuated the response to the TGFβ stimulation, and ligand treatment modestly enhanced the attenuation as shown by gene expression analysis by real-time PCR (Figure 6*C*) or Western blotting (Figure 6*D*).

To elucidate the molecular mechanism underlying the inhibitory effect of AhR on TGFβ-Smad stimulated fibrosis, we initially considered the transcriptional activity of AhR as a potential mechanism. However, the reported ChIP-seq studies showed that AhR does not bind to the consensus TGFβ-responsive element.[7, 22] Our own ChIP analysis confirmed the

lack of AhR binding to the TGFβ-responsive elements in the promoter regions of *COL1A1* and *COL1A2* genes (Supplementary Figure 8*C*). We also examined the expression of negative regulators of the TGFβ signaling pathway. There were no significant changes in the expression of genes that are known to be involved in the protein degradation (*Smurf1* and *Smurf2*), receptor antagonism (*Bambi*), nuclear transport (*Xpo1*, *Xpo4*, and *Ranbp3*), or transcriptional repressors (*Tgif*, *Ski*, and *Skil*) (Supplementary Figure 8*D*). We then determined whether AhR has a direct interaction with the Smad proteins. Co-immunoprecipitation (co-IP) analysis showed that AhR can specifically interact with Smad3, but not Smad2 or Smad4 (Figure 6*E*). The interaction did not seem to inhibit the nuclear entry of Smad2/3 (Supplementary Figure 8*E*), but at the functional level, overexpression of AhR attenuated TGFβ responsive recruitment of phosphorylated Smad3 onto the promoter regions of fibrogenic genes (Figure 6*F*).

AhR disrupts the interaction between Smad3 and β-catenin

We reason the AhR-Smad3 interaction may interfere with the accessibility of Smad3 to the Smad3-interacting transcriptional factors that are involved in ECM gene expression. Among the tested proteins β-catenin, myocyte enhancer factor 2C (MEF2C), serum response factor (SRF), and specificity protein 1 (SP1), only β-catenin exhibited substantial interaction with Smad3 in the LX2 cells (Figure 7*A*). The interaction between β-catenin and Smad3 was decreased by the overexpression of AhR and was further reduced by the TCDD treatment, which was correlated with an increased binding of Smad3 to AhR (Figure 7*B*). In contrast, the Smad3-Smad4 interaction was not affected by AhR (Figure 7*B*). We also showed that AhR decreased β-catenin's binding to Smad3 in a dose-dependent manner (Figure 7*C*), further suggesting that AhR competes with β-catenin for the binding of Smad3. Both AhR and β-catenin interact with Smad3 via the Mad homolog domain 2 (MH2) (Figure 7*D*). These results collectively suggested that AhR may attenuate TGFβ stimulated fibrosis by sequestering Smad3 from β-catenin.

β-catenin is the effector of the canonical Wnt signaling pathway that is also responsive to the TGFβ stimulation.[23] It has been reported that the coupling of Smad pathway and β-catenin is required for optimal induction of ECM gene expression and fibrogenesis.[4] However, how β-catenin potentiates TGFβ-Smad mediated fibrogenesis and whether β-catenin is the target of the anti-fibrogenic activity of AhR are unknown. We examined the kinetics of Smad2/3 phosphorylation. In the absence of AhR, overexpression of β-catenin was efficient to prolong TGFβ-stimulated Smad2/3 phosphorylation, but this effect was largely diminished by the overexpression of AhR (Figure 7*E*). At the functional level, the fibrogenic gene expression induced by β-catenin was down-regulated in primary HSCs regardless of the TGFβ treatment (Figure 7*F*).

Mechanism by which AhR facilitates the degradation of phosphorylated Smad2/3

In our effort to determine the mechanism by which AhR facilitates the degradation of phosphorylated Smad2/3, we found that treatment of LXR2 cells with MLN4924, a pan-Cullin inhibitor, abolished the inhibitory effect of AhR on the expression of fibrogenic marker genes as shown by Western blotting (Supplementary Figure 9*A*) and real-time PCR (Supplementary Figure 9*B*). This effect of MLN4924 was also confirmed in primary human

HSCs (Supplementary Figures 9*C* and *D*). These results suggested that Cullin E3 ligases may play a role in AhR-promoted degradation of phosphorylated Smad2/3. Indeed, treatment of MLN4924 or the proteasome inhibitor MG132 extended the levels of phosphorylated Smad2/3 in the presence of AhR overexpression (Supplementary Figure 9*E*). Because AhR has been reported as a component of the $CUL4B^{AhR}$ E3 ubiquitin ligase that targets the intestinal β-catenin for degradation,[12] we examined whether the E3 ligase activity of AhR is required for its inhibitory effect on HSC activation. The E3 ligase-deficient AhR mutant with the deletion of the acidic domain[12] remained effective in decreasing the expression of fibrogenic genes at the protein (Supplementary Figure 9*F*) and mRNA (Supplementary Figure 9*G*) levels, indicating that the E3 ligase activity of $CUL4B^{AhR}$ is dispensable.

Discussion

In this study, we have uncovered a novel function of AhR in HSCs and liver fibrosis. The anti-fibrogenic role of AhR in HSC activation and liver fibrosis was a surprise, because AhR has been better known for its pro-fibrogenic activity. Treatment of mice with the xenobiotic AhR activator TCDD sensitizes mice to fibrosis [13, 14, 15]. TCDD and other polycyclic aromatic hydrocarbons are known to be toxic to the hepatocytes and induce neutrophil infiltration, although the mechanism for the hepatotoxicity remains to be clearly defined. For example, the *Cyp1a1*$^{-/-}$ mice showed paradoxical protection from the toxicity of BaP[24] and TCDD[25], whereas the expression of hepatic carboxylesterase 3 (CES3) was suggested to be important for TCDD-induced liver toxicity through the production of azelaic acid monoesters[26]. Nevertheless, we speculate that the fibrogenic activity of TCDD might be secondary to its hepatotoxicity and associated inflammation, a notion that has been supported by previous reports.[27, 28] The hepatotoxicity and inflammation associated with TCDD exposure may have been exacerbated when animals were challenged with the MCD or HFD diet.[13–15] In contrast, the non-toxic endogenous AhR ligand ITE protected mice from liver fibrosis in an AhR dependent manner. TCDD and ITE share an electron rich fused aromatic ring system with a lipophilic property, suggesting both compounds can efficiently penetrate the cell membrane. However, the metabolic stability of TCDD and ITE is different, which may have contributed to their differential effect on HSC activation and liver fibrosis. TCDD is metabolically stable, with a half-life estimated to be over seven years in the human serum,[29] which renders the persistent activation of AhR. The metabolic turnover rate of endogenous AhR ligands, on the other hand, is high due to the rapid clearance by CYP1A and 1B enzymes, especially in the liver.[30] Indeed, we found the AhR-activating effect of ITE, but not TCDD, was inhibited by the co-transfection of CYP1B1 in a reporter gene assay (**data not shown**), suggesting that ITE can be metabolized by CYP1B1 while TCDD is resistant. Future studies with the use of Cyp1a and 1b knockout mice are necessary to clarify the relevance of their regulation in the fibrogenic phenotype of $AhR^{-/-}$ mice. Nevertheless, it is tempting to speculate that the “sustained” activation of AhR by xenobiotic AhR ligands such as TCDD and “transient” activation of AhR by endogenous AhR ligands such as ITE may have accounted for the differential effects between the xenobiotic and endobiotic AhR ligands.

Another interesting finding is the cell type specific role of AhR in liver fibrosis, which may have explained the counterintuitive observation that both AhR knockout and xenobiotic activation of AhR sensitized mice to liver fibrosis. The liver is an organ of multiple cell types. Most of our understanding of the hepatic function of AhR has been centered on the hepatocytes. In this study, we have presented compelling evidence that AhR is highly expressed and functional in HSCs. The expression of AhR in HSCs decreased rapidly with the onset of HSC activation, and HSCs isolated from $AhR^{-/-}$ mice exhibited increased spontaneous activation. More importantly, we showed HSC specific knockout of AhR was sufficient to cause spontaneous liver fibrosis and sensitized mice to injury induced liver fibrosis. In contrast, mice bearing hepatocyte- or Kupffer cell-specific AhR knockout did not show spontaneous liver fibrosis.

The mechanism by which AhR inhibits HSC activation was also interesting. We showed AhR impairs β-catenin-dependent stabilization of phosphorylated Smad2/3. Treatment with the ubiquitination inhibitor MLN4924 or proteasome inhibitor MG132 attenuated the inhibitory effect of AhR on Smad2/3 phosphorylation and the expression of fibrogenic genes. AhR has been reported to have E3 ligase activity.[11, 12] Interestingly, the E3-dead mutant AhR remained efficient in inhibiting HSC activation. Instead, we found AhR attenuated TGFβ-stimulated fibrogenesis by interacting with Smad3, which may have sequestered Smad3 from interacting with β-catenin. TGFβ is known to be pro-fibrogenic in HSCs and Smad3 is a key effector of the TGFβ signaling. The canonical Wnt signaling and its down-stream effector β-catenin have been suggested to play a role in fibrotic responses.[4] Indeed, our RNA-seq results showed an up-regulation of both the Wnt and TGFβ pathways in $AhR^{-/-}$ HSCs. Our results suggested that β-catenin stabilizes the transcriptionally active phosphorylated Smad2/3. It has been reported that β-catenin interacts with the C-terminal MH2 domain of Smad3.[31] This MH2 domain is also the binding site for E3 ligases.[32] Therefore, it is reasonable to speculate that the stabilization of phosphorylated Smad2/3 protein by β-catenin could have been achieved through the prevention of ubiquitination. The E3 ligase responsible for AhR dependent destabilization of phosphorylated Smad2/3 remains to be defined. The AhR-Smad3 interaction and the sequestration of Smad3 from β-catenin suggest a plausible mechanism by which AhR inhibits HSC activation and liver fibrosis. Although our RNA-seq results suggested AhR may not directly inhibit HSC activation as a genomic repressor of the fibrogenic genes, we cannot exclude the transcriptional role of AhR as a mechanism to prevent HSC activation. It remains possible that certain AhR-regulated genes play a role in mediating the anti-fibrogenic effect of AhR.

Among limitations, much of our mechanistic characterization was in vitro studies. Previous reports suggested that the TGFβ-Smad pathway was activated in $AhR^{-/-}$ mice,[34, 35] which was consistent with our results. However, future studies are necessary to determine whether fibrosis caused by AhR knockout requires the TGFβ-Smad signaling in vivo and in HSCs by using *Ctnnb1* and *Smad2/¾* floxed mice. In addition, it is unclear whether AhR-regulated Smad3-β-catenin interaction is also applicable in other biological events, such as embryonic stem cell differentiation (Supplementary Table 7).

In summary, we have established AhR as an anti-fibrogenic transcriptional factor in HSCs. Our results strongly suggest that development of non-toxic AHR agonists and strategies that

preferentially activate AhR in HSCs may represent novel approaches to prevent and treat liver fibrosis.

Supplementary Material

Refer to Web version on PubMed Central for supplementary material.

Acknowledgements

We thank Dr. Jodi A. Flaws (University of Illinois Urbana-Champaign, Urbana, IL) for the Ad-AhR and control Ad-GFP adenovirus, and Dr. Tong-Chuan He (University of Chicago, Chicago, IL) for the Ad-β-catenin (S33Y).

Funding Statement: This work was supported in part by NIH grants DK083952 and ES023438 to WX.

References

1. Bataller R, Brenner DA. Liver fibrosis. J Clin Invest 2005;115:209–18. [PubMed: 15690074]
2. Mederacke I, Hsu CC, Troeger JS, et al. Fate tracing reveals hepatic stellate cells as dominant contributors to liver fibrosis independent of its aetiology. Nat Commun 2013;4:2823. [PubMed: 24264436]
3. Tsuchida T, Friedman SL. Mechanisms of hepatic stellate cell activation. Nat Rev Gastroenterol Hepatol 2017;14:397–411. [PubMed: 28487545]
4. Akhmetshina A, Palumbo K, Dees C, et al. Activation of canonical Wnt signalling is required for TGF-β-mediated fibrosis. Nat Commun 2012;3:735. [PubMed: 22415826]
5. Beischlag TV, Morales JL, Hollingshead BD, et al. The aryl hydrocarbon receptor complex and the control of gene expression. Crit Rev Eukaryot Gene Expr 2008;18:207–50. [PubMed: 18540824]
6. Jackson D, Joshi A, Elferink C. Ah receptor pathway intricacies; signaling through diverse protein partners and DNA-motifs. Toxicol Res 2015;4:1143–1158.
7. Lo R, Matthews J. High-resolution genome-wide mapping of AHR and ARNT binding sites by ChIP-Seq. Toxicol Sci 2012;130:349–61. [PubMed: 22903824]
8. Fernandez-Salguero P, Pineau T, Hilbert DM, et al. Immune system impairment and hepatic fibrosis in mice lacking the dioxin-binding Ah receptor. Science 1995;268:722–726. [PubMed: 7732381]
9. Schmidt JV, Su G, Reddy JK, et al. Characterization of a murine Ahr null allele: involvement of the Ah receptor in hepatic growth and development. Proc Natl Acad Sci U S A 1996;93:6731–6736. [PubMed: 8692887]
10. Nebert DW. Aryl hydrocarbon receptor (AHR):“pio neer member” of the basic-helix/loop/helix per-Arnt-sim (bHLH/PAS) family of “sensors” of foreign and endogenous signals. Prog Lipid Res 2017;67:38–57. [PubMed: 28606467]
11. Ohtake F, Baba A, Takada I, et al. Dioxin receptor is a ligand-dependent E3 ubiquitin ligase. Nature 2007;446:562–566. [PubMed: 17392787]
12. Kawajiri K, Kobayashi Y, Ohtake F, et al. Aryl hydrocarbon receptor suppresses intestinal carcinogenesis in ApcMin/+ mice with natural ligands. Proc Natl Acad Sci U S A 2009;106:13481–13486. [PubMed: 19651607]
13. He J, Hu B, Shi X, et al. Activation of the aryl hydrocarbon receptor sensitizes mice to nonalcoholic steatohepatitis by deactivating mitochondrial sirtuin deacetylase Sirt3. Mol Cell Biol 2013;33:2047–2055. [PubMed: 23508103]
14. Pierre S, Chevallier A, Teixeira-Clerc F, et al. Aryl hydrocarbon receptor–dependent induction of liver fibrosis by dioxin. Toxicol Sci 2014;137:114–124. [PubMed: 24154488]
15. Duval C, Teixeira-Clerc F, Leblanc AF, et al. Chronic exposure to low doses of dioxin promotes liver fibrosis development in the C57BL/6J diet-induced obesity mouse model. Environ Health Perspect 2017;125:428–436. [PubMed: 27713108]
16. Mederacke I, Dapito DH, Affò S, et al. High-yie ld and high-purity isolation of hepatic stellate cells from normal and fibrotic mouse livers. Nat Protoc 2015;10:305–315. [PubMed: 25612230]

17. Subramanian A, Tamayo P, Mootha VK, et al. Gene set enrichment analysis: a knowledge-based approach for interpreting genome-wide expression profiles. Proc Natl Acad Sci U S A 2005;102:15545–50. [PubMed: 16199517]
18. Gao J, Yan J, Xu M, et al. CAR suppresses hepatic gluconeogenesis by facilitating the ubiquitination and degradation of PGC1α. Mol Endocrinol 2015;29:1558–1570. [PubMed: 26407237]
19. Song J, Clagett-Dame M, Peterson RE, et al. A ligand for the aryl hydrocarbon receptor isolated from lung. Proc Natl Acad Sci U S A 2002;99:14694–14699. [PubMed: 12409613]
20. Walisser JA, Glover E, Pande K, et al. Aryl hydrocarbon receptor-dependent liver development and hepatotoxicity are mediated by different cell types. Proc Natl Acad Sci U S A 2005;102:17858–17863. [PubMed: 16301529]
21. Azimifar SB, Nagaraj N, Cox J, et al. Cell-type-resolved quantitative proteomics of murine liver. Cell Metab 2014;20:1076–1087. [PubMed: 25470552]
22. Dere E, Lo R, Celius T, et al. Integration of genome-wide computation DRE search, AhR ChIP-chip and gene expression analyses of TCDD-elicited responses in the mouse liver. BMC Genomics 2011;12:365. [PubMed: 21762485]
23. Jian H, Shen X, Liu I, et al. Smad3-dependent nuclear translocation of beta-catenin is required for TGF-beta1-induced proliferation of bone marrow-derived adult human mesenchymal stem cells. Genes Dev 2006;20:666–74. [PubMed: 16543220]
24. Uno S, Dalton TP, Shertzer HG, et al. Benzo[a]pyrene-induced toxicity: paradoxical protection in Cyp1a1(−/−) knockout mice having increased hepatic BaP-DNA adduct levels. Biochem Biophys Res Commun 2001;289:1049–56. [PubMed: 11741297]
25. Uno S, Dalton TP, Sinclair PR, et al. Cyp1a1(−/−) male mice: protection against high-dose TCDD-induced lethality and wasting syndrome, and resistance to intrahepatocyte lipid accumulation and uroporphyria. Toxicol Appl Pharmacol 2004;196:410–21. [PubMed: 15094312]
26. Matsubara T, Tanaka N, Krausz KW, et al. Metabolomics identifies an inflammatory cascade involved in dioxin- and diet-induced steatohepatitis. Cell Metab 2012;16:634–44. [PubMed: 23140643]
27. Ozeki J, Uno S, Ogura M, et al. Aryl hydrocarbon receptor ligand 2,3,7,8-tetrachlorodibenzo-p-dioxin enhances liver damage in bile duct-ligated mice. Toxicology 2011;280:10–7. [PubMed: 21095216]
28. Lamb CL, Cholico GN, Pu X, et al. 2,3,7,8-Tetrachlorodibenzo-p-dioxin (TCDD) increases necroinflammation and hepatic stellate cell activation but does not exacerbate experimental liver fibrosis in mice. Toxicol Appl Pharmacol 2016;311:42–51. [PubMed: 27693115]
29. Pirkle JL, Wolfe WH, Patterson DG, et al. Estimates of the half-life of 2, 3, 7, 8-tetrachlorodibenzo-p-dioxin in Vietnam veterans of Operation Ranch Hand. Journal of Toxicology and Environmental Health, Part A Current Issues 1989;27:165–171.
30. Wincent E, Bengtsson J, Bardbori AM, et al. Inhibition of cytochrome P4501-dependent clearance of the endogenous agonist FICZ as a mechanism for activation of the aryl hydrocarbon receptor. Proceedings of the National Academy of Sciences 2012;109:4479–4484.
31. Zhang M, Wang M, Tan X, et al. Smad3 prevents β-catenin degradation and facilitates β-catenin nuclear translocation in chondrocytes. J Biol Chem 2010;285:8703–8710. [PubMed: 20097766]
32. Gao S, Alarcón C, Sapkota G, et al. Ubiquitin l igase Nedd4L targets activated Smad2/3 to limit TGF-β signaling. Mol Cell 2009;36:457–468. [PubMed: 19917253]
33. Dere E, Forgacs AL, Zacharewski TR, et al. Genome-wide computational analysis of dioxin response element location and distribution in the human, mouse, and rat genomes. Chem Res Toxicol 2011;24:494–504. [PubMed: 21370876]
34. Corchero J, Martin-Partido G, Dallas SL, et al. Liver portal fibrosis in dioxin receptor-null mice that overexpress the latent transforming growth factor-beta-binding protein-1. Int J Exp Pathol 2004;85:295–302. [PubMed: 15379962]
35. Andreola F, Calvisi DF, Elizondo G, et al. Reversal of liver fibrosis in aryl hydrocarbon receptor null mice by dietary vitamin A depletion. Hepatology 2004;39:157–66. [PubMed: 14752834]

What You Need to Know

Background and Context:

The liver contains multiple cell types. We investigated how the expression of aryl hydrocarbon receptor (AHR) by different cell types affects liver fibrosis and activation of hepatic stellate cells (HSCs) in mice.

New Findings:

AHR signaling prevents activation of HSCs and expression of genes required for liver fibrogenesis.

Limitations:

Although human HSCs were used and bioinformatic analyses were performed on human liver samples, more human studies will further enhance the human relevance.

Impact:

Non-toxic AHR agonists or strategies to activate AHR signaling in HSCs might be developed to prevent or treat liver fibrosis.

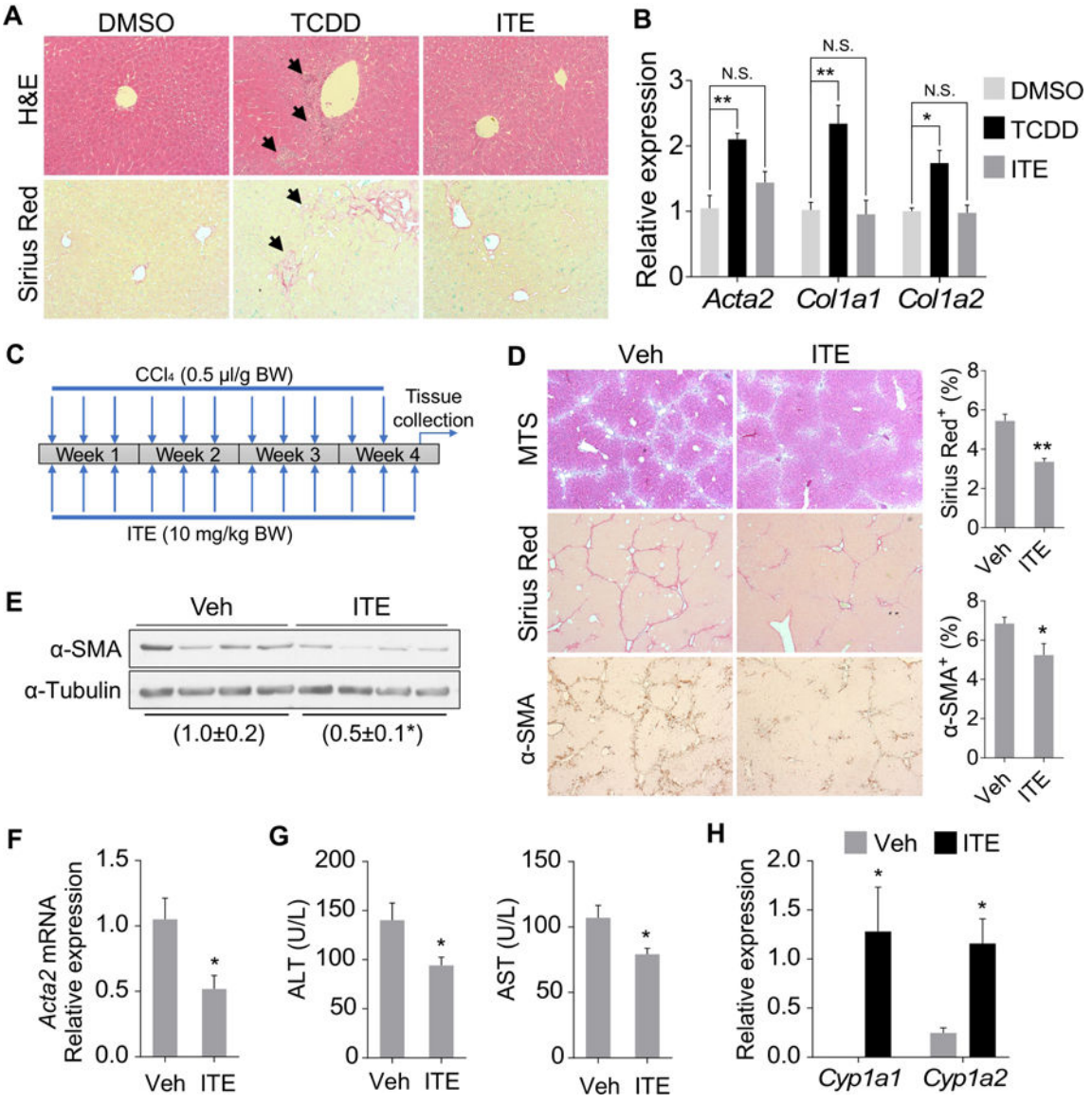

Figure 1. Treatment of mice with the non-toxic AhR ligand ITE ameliorates CCl_4-induced liver fibrosis.

(A and B) Six week old male C57BL/6J mice were treated with vehicle (DMSO), TCDD (25 μg/kg), or ITE (10 mg/kg) once a week for two weeks (n=4 per group) before being analyzed for histology by H&E and Sirius Red staining (A, original magnification 20X) and the expression of fibrogenic genes by real-time PCR (B). Arrows indicate neutrophil infiltration in H&E and collagen deposition in the Sirius Red staining. **(C-H)** Eight week old male C57BL/6J mice were treated with vehicle or ITE (10 mg/kg) together with CCl_4 (0.5 μl/g body weight) three times a week for four weeks (n=6 per group) as outlined in (C). Histology was analyzed by Masson's Trichrome staining (MTS), Sirius Red staining, and α-SMA immunostaining (D, original magnification 5X) with the quantification of Sirius Red and α-SMA staining shown on the right. The hepatic protein (E) and mRNA (F) expression of α-SMA was measured by Western blotting and real-time PCR, respectively. The serum levels of ALT and AST (G) and the hepatic expression of *Cyp1a1* and *Cyp1a2* (H) were also

measured. All data were presented as mean ± SEM. *, $p<0.05$; **, $p<0.01$; N.S., statistically not significant.

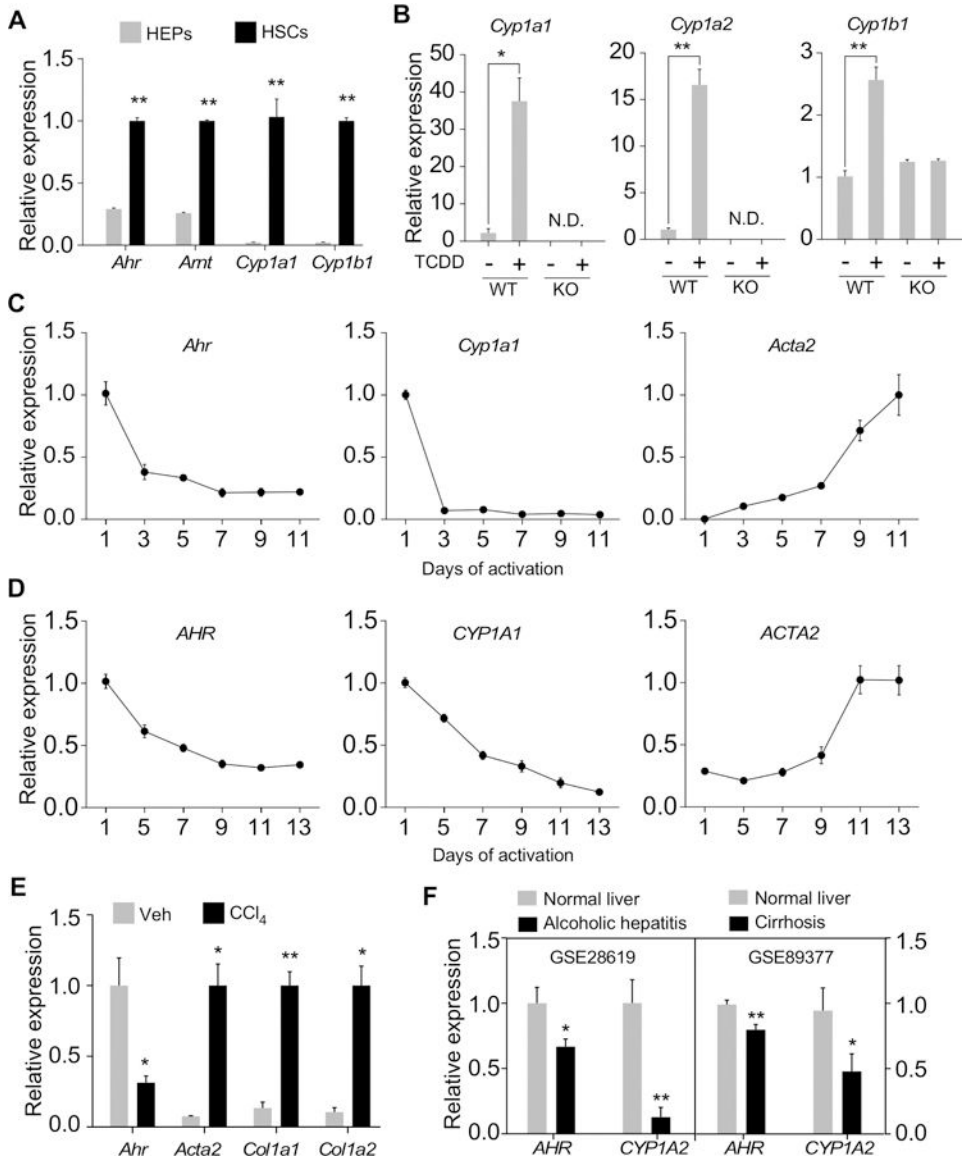

Figure 2. AhR is highly expressed in HSCs and the expression of AhR inversely correlates with HSC activation.

(A) Primary hepatocytes (HEPs) and HSCs were isolated from the same mouse liver. Gene expression was determined immediately after cell isolation by real-time PCR (n=4). **(B)** Primary HSCs were isolated from WT or $AhR^{-/-}$ (KO) mice and treated with TCDD (20 nM) for 6 days. Gene expression was determined by real-time PCR (n=4). **(C and D)** Primary mouse (C) or human (D) HSCs were culture-activated for the indicated duration. Gene expression was determined by real-time PCR (n=4). **(E)** Primary mouse HSCs were isolated from male mice treated with four doses of CCl_4 (0.5 μl/g body weight, every 3 days, n=3) or vehicle (n=4). Gene expression was determined immediately after cell isolation by real-time PCR. **(F)** Two datasets (GSE28619 and GSE89377) from the GEO database were analyzed for the expression of *AHR* and *CYP1A2*. All data were presented as mean ± SEM. *, $p<0.05$; **, $p<0.01$; N.D., not detectable.

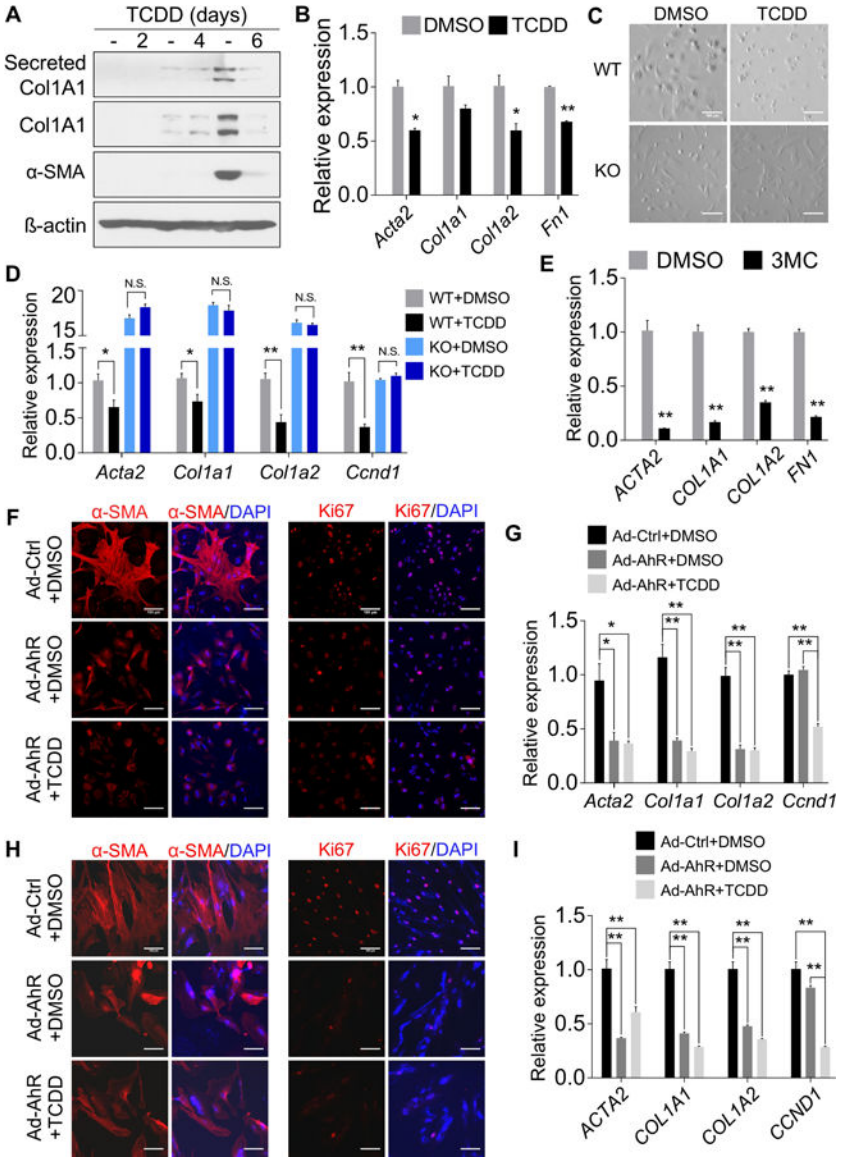

Figure 3. Pharmacological activation or forced expression of AhR inhibits HSC activation.

(A) Primary mouse HSCs were treated with TCDD (50 nM) for 2, 4, and 6 days, respectively. Protein levels from the culture medium or whole cell lysates were detected by Western blotting. **(B)** Primary mouse HSCs were treated with TCDD (20 nM) for 4 days. Gene expression was determined by real-time PCR (n=3). **(C and D)** Primary mouse HSCs were isolated from WT and $AhR^{-/-}$ mice and treated with TCDD (20 nM) for 6 days. Cell morphology was analyzed by light field microscopy (C) and gene expression was determined by real-time PCR (D, n=4). **(E)** Primary human HSCs were treated with 3MC (2 μM) for 6 days. Gene expression was determined by real-time PCR (n=4). **(F and G)** Primary mouse HSCs were infected with adenovirus overexpressing AhR (MOI=10) and treated with or without TCDD (50 nM). The expression of α-SMA and Ki67 was detected by immunofluorescence (F), and gene expression was determined by real-time PCR (G, n=3). **(H and I)** The experiments were the same as in (F and G) except that primary human

HSCs were used. Scale bar=100 μm. All data were presented as mean ± SEM. *, $p<0.05$; **, $p<0.01$.

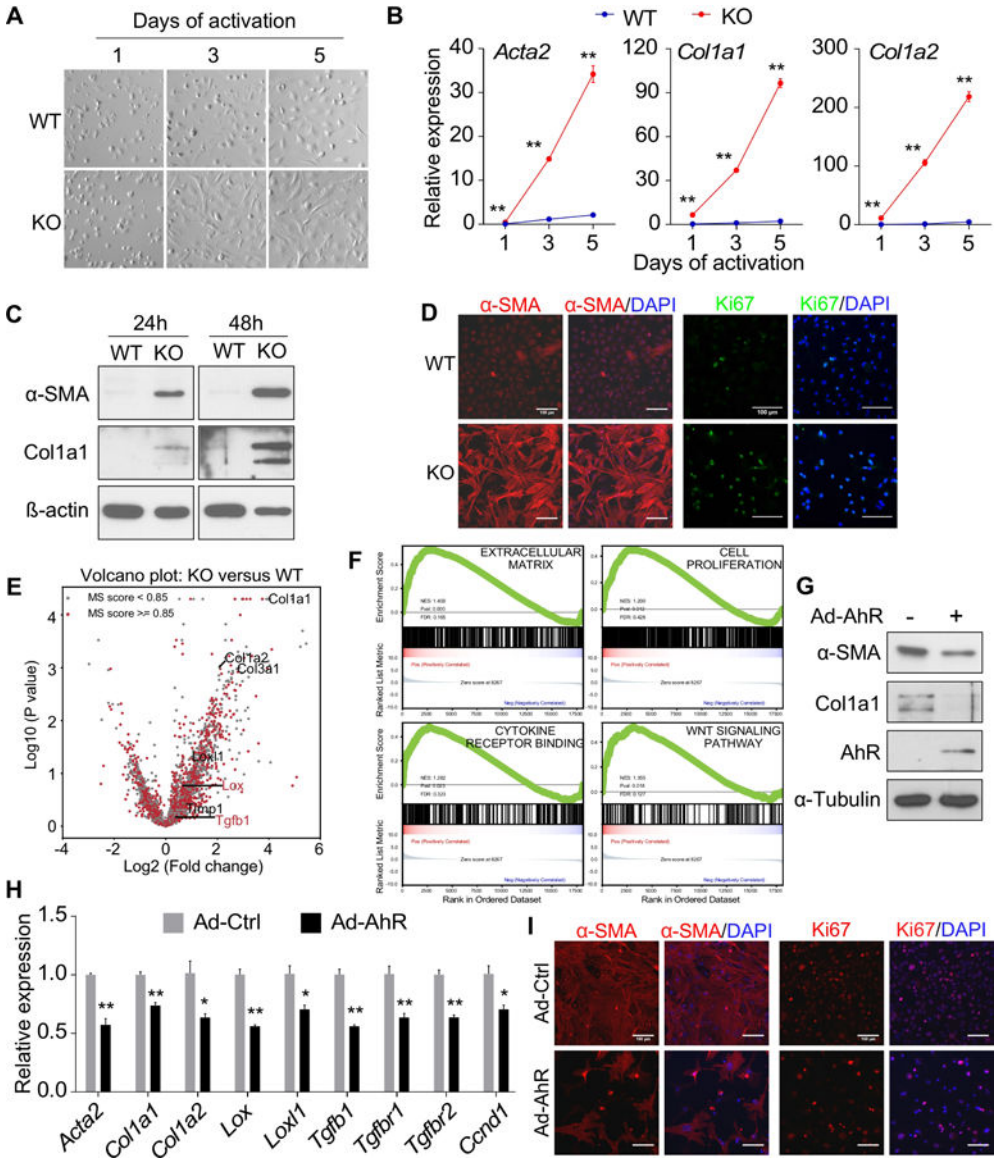

Figure 4. Knockout of AhR promotes HSC activation in vitro.

(A and B) Primary mouse HSCs were isolated from WT and AhR$^{-/-}$ (KO) mice and culture-activated for the indicated duration. Cell morphology was analyzed by light field microscopy (A) and gene expression was determined by real-time PCR (B, n=4). **(C)** Primary mouse HSCs were isolated and culture-activated for 24h or 48h. The protein expression was determined by Western blotting. **(D)** Primary mouse HSCs were isolated and culture-activated for 48h. The expression of α-SMA and Ki67 was detected by immunofluorescence. **(E)** Primary mouse HSCs were isolated and FACS purified and directly subject to RNA-seq analysis. Differentially expressed genes are shown by a volcano plot with several fibrogenic marker genes annotated. The red dots and blue dots indicate genes that are significantly up-regulated (663 genes) and down-regulated (66 genes), respectively. The cutoff was set as 0.05 for p-value and 1.5 for log2(FC) (FC: fold change, KO versus WT). **(F)** Gene set enrichment analysis (GSEA) of the RNA-seq results. **(G-I)**

Primary mouse HSCs isolated from KO mice were infected with adenovirus overexpressing AhR and treated with or without TCDD (50 nM). The gene expression was determined by Western blotting (G), real-time PCR (H, n=4), or immunofluorescence (I). Scale bar=100 μm. All data were presented as mean ± SEM. *, $p<0.05$; **, $p<0.01$.

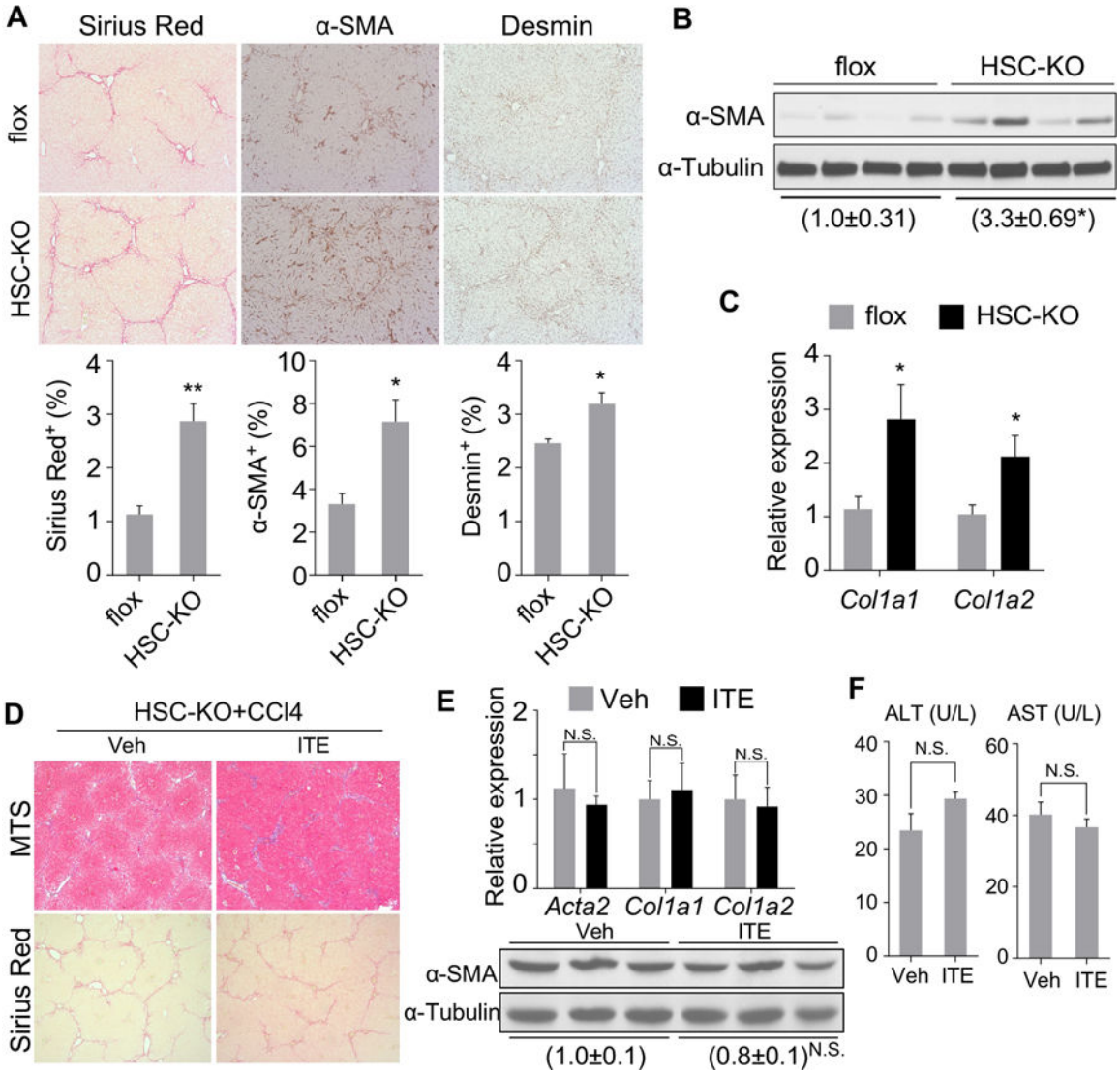

Figure 5. Knockout of AhR in HSCs sensitizes mice to liver fibrosis and abolishes the anti-fibrotic activity of ITE.

(A-C) 9–10 week old male $AhR^{flox/flox}$ (flox) and HSC-KO mice were treated with CCl_4 (1 μl/g body weight) twice a week for 4 weeks (n=5 per group). The liver histology was analyzed by Sirius Red staining and immunostaining of α-SMA and Desmin (A, original magnification 10X with the quantifications of staining shown on the bottom). The α-SMA protein level was determined by Western blotting (B), and the mRNA expression of *Col1a1* and *Col1a2* was determined by real-time PCR (C). **(D-F)** 8–10 week old male HSC-KO mice were treated with vehicle or ITE (10 mg/kg) together with CCl_4 (0.5 μl/g body weight) three times a week for four weeks (n=3 per group). Liver tissues were analyzed for histology by Masson's Trichrome (MTS) and Sirius Red staining (D, original magnification 5X), the expression of fibrogenic gene by real-time PCR (top) or Western blotting (bottom) (E), and the serum ALT and AST levels (F). All data were presented as mean ± SEM. *, $p<0.05$; **, $p<0.01$; N.S., statistically not significant.

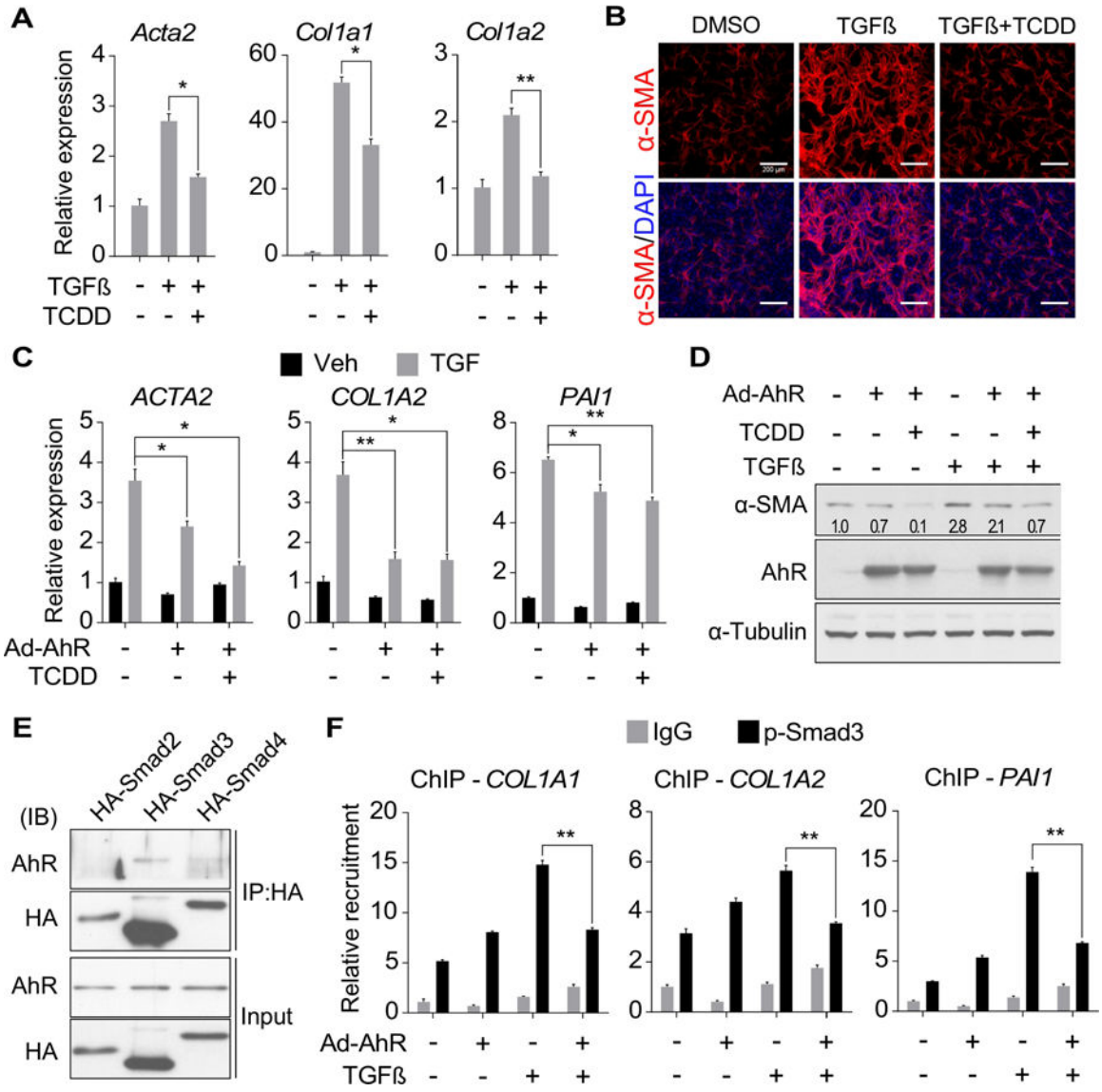

Figure 6. AhR attenuates TGFβ-stimulated fibrogenesis by inhibiting Smad3-mediated transcriptional activation of fibrogenic genes.

(A) Primary mouse HSCs were treated with TGFβ1 (2 ng/ml) in the absence or presence of TCDD (50 nM) for 24h. Gene expression was determined by real-time PCR (n=3). **(B)** Primary mouse HSCs were treated with TGFβ1 (2 ng/ml) in the absence or presence of TCDD (50 nM) for 48h. The expression of α-SMA was determined by immunofluorescence. Scale bar=200 μm. **(C and D)** LX2 cells were infected with adenovirus overexpressing AhR and treated with TCDD (50 nM) and/or TGFβ1 (5 ng/ml) for 24h. The gene expression at mRNA (C) and protein (D) levels were measured by real-time PCR (n=4) and Western blotting, respectively. The relative values of α-SMA protein expression in the Western blotting are labeled. **(E)** LX2 cells stably expressing human AhR were transfected with HA-Smad2, HA-Smad3, or HA-Smad4 expression vector. Protein interaction was determined by co-immunoprecipitation with an HA antibody followed by Western blotting. **(F)** LX2 cells infected with adenovirus overexpressing AhR were pre-treated with or without TCDD (50

nM) for 24h and then TGFβ1 (5 ng/ml) with or without TCDD (50 nM) for 4h. The recruitment of phosphorylated Smad3 onto the promoter regions of the *COL1A1*, *COL1A2* and *PAI1* genes were determined by ChIP coupled with real-time PCR on the recovered DNA (n=4). All data were presented as mean ± SEM. *, $p<0.05$; **, $p<0.01$.

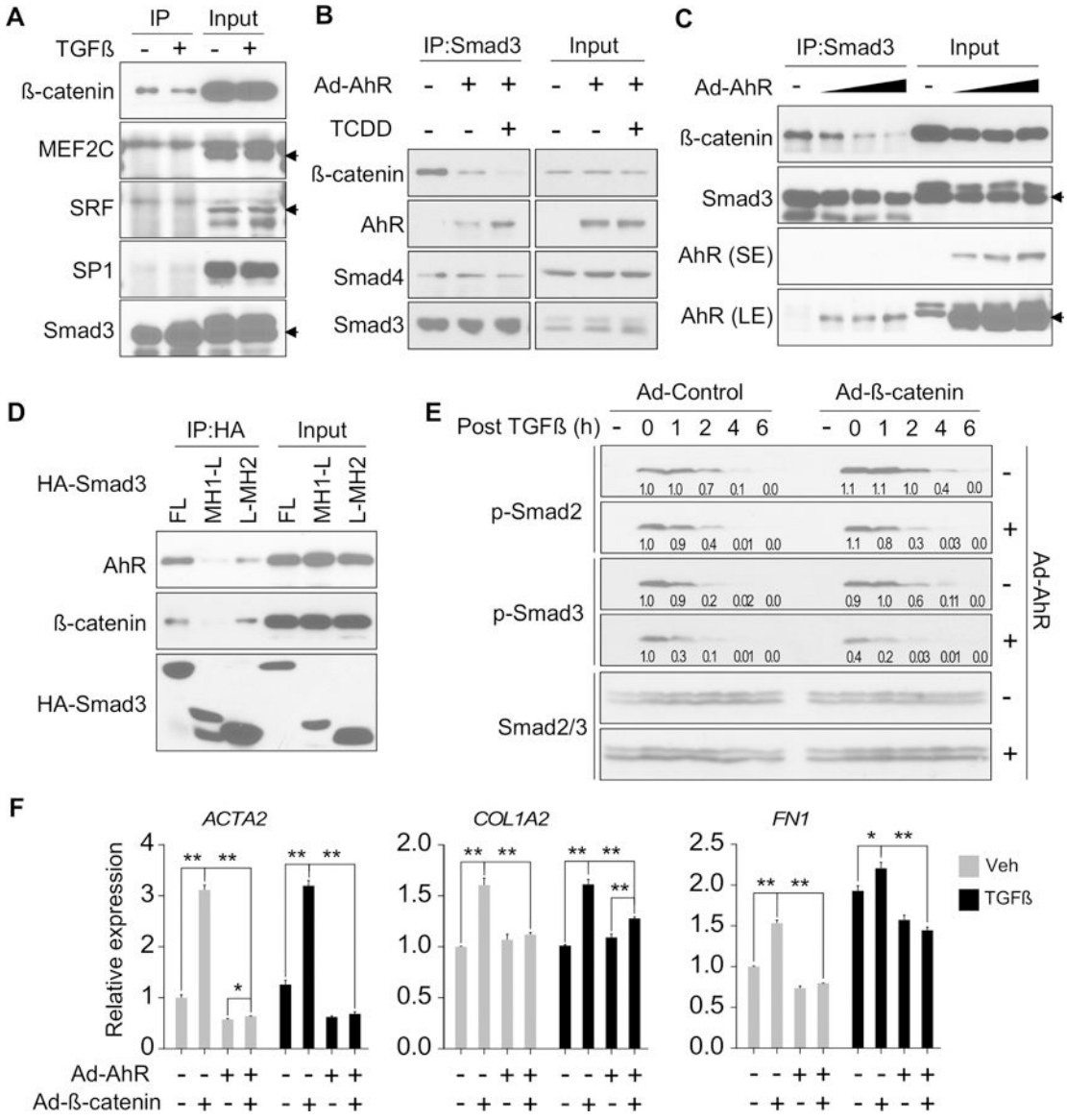

Figure 7. AhR disrupts the interaction between Smad3 and β-catenin.

(A) LX2 cells were stimulated with TGFβ1 (5 ng/ml) for 3h. Protein interaction was determined by co-immunoprecipitation with an anti-Smad3 antibody followed by Western blotting. Arrows indicate the specific protein bands. **(B)** LX2 cells were infected with adenovirus overexpressing AhR and treated with or without TCDD (50 nM). Protein interaction was determined by co-immunoprecipitation with an anti-Smad3 antibody. **(C)** LX2 were infected with increasing doses of Ad-AhR. Protein interaction was determined by co-immunoprecipitation with an anti-Smad3 antibody. Arrows indicate the specific protein bands. SE and LE indicate short exposure and long exposure, respectively. **(D)** LX2 cells stably transfected with AhR were transiently transfected with HA-Smad3 plasmids (FL, full-length; MH1-L, MH1 domain plus linker; L-MH2, linker plus MH2 domain). Protein interaction was determined by co-immunoprecipitation with an anti-HA antibody. **(E)** LX2 were infected with Ad-AhR and/or Ad-β-catenin, and then stimulated with TGFβ1 (5 ng/ml)

for 1h before harvesting at indicated time points. The levels of phosphorylated Smad2/3 were detected by Western blotting with the relative quantitative values labeled. **(F)** Primary human HSCs were infected with Ad-AhR with or without Ad-β-catenin and treated with TCDD (50 nM) and TGFβ1 (5 ng/ml) as indicated. Gene expression was determined by real-time PCR. All data were presented as mean ± SEM. *, $p<0.05$; **, $p<0.01$.